Molecular Cell
Article

Tet Proteins Connect the O-Linked N-acetylglucosamine Transferase Ogt to Chromatin in Embryonic Stem Cells

Pietro Vella,[1,6] Andrea Scelfo,[1,6] SriGanesh Jammula,[1] Fulvio Chiacchiera,[1] Kristine Williams,[2,3] Alessandro Cuomo,[1] Alessandra Roberto,[1,5] Jesper Christensen,[2,3] Tiziana Bonaldi,[1] Kristian Helin,[2,3,4] and Diego Pasini[1,*]
[1]Department of Experimental Oncology, European Institute of Oncology, Via Adamello 16, 20139 Milan, Italy
[2]Biotech Research and Innovation Centre
[3]Centre for Epigenetics
University of Copenhagen, Ole Maaløes Vej 5, 2200 Copenhagen, Denmark
[4]The Danish Stem Cell Centre, University of Copenhagen, Blegdamsvej 3, 2200 Copenhagen, Denmark
[5]Present address: Laboratory of Clinical and Experimental Immunology, Humanitas Clinical and Research Center, Via Manzoni 56, 20089 Rozzano MI, Italy
[6]These authors contributed equally to this work
*Correspondence: diego.pasini@ieo.eu
http://dx.doi.org/10.1016/j.molcel.2012.12.019

SUMMARY

O-linked N-acetylglucosamine (O-GlcNAc) transferase (Ogt) activity is essential for embryonic stem cell (ESC) viability and mouse development. Ogt is present both in the cytoplasm and the nucleus of different cell types and catalyzes serine and threonine glycosylation. We have characterized the biochemical features of nuclear Ogt and identified the ten-eleven translocation (TET) proteins Tet1 and Tet2 as stable partners of Ogt in the nucleus of ESCs. We show at a genome-wide level that Ogt preferentially associates with Tet1 to genes promoters in close proximity of CpG-rich transcription start sites. These regions are characterized by low levels of DNA modification, suggesting a link between Tet1 and Ogt activities in regulating CpG island methylation. Finally, we show that Tet1 is required for binding of Ogt to chromatin affecting Tet1 activity. Taken together, our data characterize how O-GlcNAcylation is recruited to chromatin and interacts with the activity of 5-methylcytosine hydroxylases.

INTRODUCTION

The O-linked N-acetylglucosamine (O-GlcNAc) transferase Ogt is an evolutionarily conserved enzyme that catalyzes all O-linked protein glycosylation (Haltiwanger et al., 1992). OGT is present in both the cytoplasm and the nucleus of cells and modifies threonine and serine residues through the attachment of an N-acetyl glucosamine moiety to their hydroxyl groups (Haltiwanger et al., 1992; Holt and Hart, 1986). The *Ogt* gene locus resides on the X chromosome and its activity is required for the viability of male embryonic stem cells (ESCs) (Shafi et al., 2000). Consistent with this, *Ogt* knockout (KO) mice are not viable and die during embryogenesis. Moreover, maternal loss of Ogt results in lack of viability of heterozygous embryos no later than day 5 postcoitus due to developmental defects of the extra embryonic tissues that are engaged by paternal X chromosome inactivation (Shafi et al., 2000).

Over the past 15 years, several different Ogt substrates have been identified, suggesting that Ogt can control different cellular functions in agreement with the severe phenotypes observed upon loss of Ogt activity (Love and Hanover, 2005; Vosseller et al., 2001). O-linked protein glycosylation is counteracted by the activity of the O-GlcNAcase OGA that actively removes O-GlcNAc groups from O-glycosylated proteins (Gao et al., 2001). OGT and OGA are the final executors of hexosamine signaling (HSP), a metabolic pathway that senses the nutrient state of the cells. O-GlcNAc is produced from glucose, glutamine, acetyl-CoA, uridine, and ATP, and reduced levels of O-GlcNAc inhibit proteins' O-linked glycosylation, making OGT and OGA potent nutrient sensors (Love and Hanover, 2005). Importantly, HSP and in particular OGA and OGT activities have been directly linked to the insulin resistance that is acquired in patients with diabetes mellitus (Love and Hanover, 2005). For example, the overexpression of OGT in muscle and fat tissue leads to the development of type II diabetes in mice (McClain et al., 2002). In addition, alterations in protein O-GlcNAcylation have been directly linked to other aging related diseases such as cancer and neurodegenerative disorders (Hart et al., 2011; Love and Hanover, 2005). In this latter case, the progression of neural degeneration, which is also related to an acquisition of insulin resistance by the patients, has been directly associated to a deregulated OGT activity (Love and Hanover, 2005).

While in the cytoplasm OGT glycosylates several proteins like proteasome components, chaperones, and kinases, in the nucleus OGT was shown to modify important transcriptional regulators such as the transcription factors SP1, HCFC1, MYC, p53, and Oct4 as well as the C-terminal domain (CTD) of RNA polymerase II (RNApol-II) (Capotosti et al., 2011; Chou et al., 1995; Comer and Hart, 2001; Jackson and Tjian, 1988; Jang et al., 2012; Shaw et al., 1996). In general, one of the most accepted functions for O-glycosylation is to prevent proteins

phosphorylation (Zeidan and Hart, 2010). For example, RNApol-II glycosylation mainly occurs at the threonine 4 residue of the CTD repeats and has been suggested to counteract CTD phosphorylation, hence inhibiting RNApol-II activation and elongation (Comer and Hart, 2001). Differently, OGT dependent O-GlcNAcylation induces cleavage of the transcription factor HCFC1, regulating its related cell-cycle control (Capotosti et al., 2011), and the activity of Oct4 in maintaining ESC pluripotency (Jang et al., 2012).

Recent findings also identified several histone proteins as targets of O-linked glycosylation. General O-GlcNAcylation has been reported for histone H2B, H3, and H4 (Sakabe et al., 2010), while the specific glycosylation of histone H2B at serine 112 (H2Bgly) was shown to favor the ubiquitylation of lysine (K) 120 of the same histone (H2Bubq), thus promoting transcriptional elongation (Fujiki et al., 2011). Overall, these latest findings strongly suggest that nutrient metabolism could act directly in shaping cells epigenetic landscape.

Due to the multiple essential functions of Ogt, we decided to characterize the biochemical features of nuclear Ogt by performing a tandem protein complex purification from ESCs. This approach allowed us to identify two components of the ten-eleven translocation (TET) protein family, Tet1 and Tet2, as stable partners of Ogt in the ESC nucleus. The TET proteins belong to a family of dioxygenases that catalyze the hydroxylation of 5-methylcytosine (5hmC and 5mC, respectively) (Wu and Zhang, 2011). Depletion of TET proteins levels results in loss of 5hmC (Dawlaty et al., 2011; Ito et al., 2010; Koh et al., 2011; Tahiliani et al., 2009; Wu et al., 2011b). TET1 and TET2 are highly expressed in ESCs, while TET3 is active at early stages of embryogenesis and regulates postfertilization paternal DNA reprogramming through loss of DNA methylation (Gu et al., 2011; Inoue and Zhang, 2011). In ESCs, TET1 associates both to promoters and to distal regulatory elements (Ficz et al., 2011; Williams et al., 2011; Wu et al., 2011b). While 5mC is excluded from CpG-rich promoter regions, 5hmC DNA immunoprecipitation (hmeDIP) analyses have shown that 5hmC can accumulates at promoters with higher CpG content (Williams et al., 2011; Wu et al., 2011a; Xu et al., 2011). Recent sequencing approaches resolved the single-base 5mC and 5hmC genome-wide modification map of ESCs showing that, despite the fact that some CpG islands retain substantial enrichment of 5hmC, most of the 5hmC sites (~46%) reside at regulatory elements in proximity of transcription factor (TF) DNA binding sites (Booth et al., 2012; Yu et al., 2012). Interestingly, differently from 5mC, 5hmC deposition seems to accumulate asymmetrically respect to the anti-parallel DNA filaments (Yu et al., 2012). Hydroxylation of 5mC has been proposed to promote passive or DNA repair-dependent loss of cytosine methylation, a mechanism that is consistent with the low level of DNA modifications that are detected at TET1 bound promoters (Wu and Zhang, 2011). This correlation led to the speculation that TETs' activity might serve as a fidelity mechanism that allows maintaining CpG-rich DNA elements free of DNA methylation (Williams et al., 2012). Thus, the identification of a potential complex between Ogt, Tet1, and Tet2 encouraged us to further characterize this functional interaction leading to the discovery that Tet1 regulates Ogt recruitment to gene transcription start sites regulating its chromatin related activities.

RESULTS

Tet1 and Tet2 Stably Interact with Ogt

In order to identify interacting partners of Ogt in the nucleus of ESCs, we generated a stable ESC line that expresses a flag-tagged biotinylated form of Ogt (fbio-Ogt) in cells that constitutively express the BirA enzyme (BirA-ES). With this approach, we have previously obtained efficient in vivo protein biotinylation (Vella et al., 2012). We have selected a BirA-ES clone that expresses subphysiological levels of fbio-Ogt and that retains efficient Ogt in vivo biotinylation (Figure 1A). Since Ogt is present in both the cytoplasm and in the nucleus of different cell types (Kreppel et al., 1997), we tested whether fbio-Ogt has a comparable cellular localization to endogenous Ogt. For this purpose, we have fractionated the nucleus and the cytoplasm of fbio-Ogt BirA ESCs by hypotonic extraction and analyzed the localization of fbio-Ogt relative to its endogenous counterpart. The western blot (WB) analysis presented in Figure 1B demonstrates that endogenous and fbio-Ogt have a comparable cellular localization. With these cells, we have tested the extractability of Ogt by preparing nuclear protein extracts that have been lysed at different salt concentrations. As shown in Figure S1A (available online), maximum Ogt chromatin extraction was obtained at 300 mM NaCl concentration. This condition was chosen to prepare nuclear protein extracts in order to identify fbio-Ogt-interacting proteins. Thus, we have performed a tandem flag and Streptavidin affinity purification using nuclear extracts from both control and fbio-Ogt BirA ESCs (Figure 1C). The eluted proteins have been separated and silver stained on a polyacrylamide denaturing gel showing that fbio-Ogt purification specifically enriched several additional proteins (Figure 1C). Analysis by mass spectrometry (MS/MS) of the eluted material led to the identification of previously known Ogt-interacting proteins like Hcfc1 or Sin3a (Chou et al., 1995; Yang et al., 2002), demonstrating the strength of our approach (Figure 1D). Moreover, among the most enriched fbio-Ogt purified proteins, the MS analyses identified also two components of the ten eleven-translocation protein family that are expressed in ESCs, Tet1 and Tet2 (Figure 1D). Interestingly, Sin3a was previously shown to interact with both Hdac1 and Tet1 (Hassig et al., 1997; Williams et al., 2012), and the finding that Ogt also copurify the same proteins potentially suggests the existence of a complex containing Ogt, Sin3a, Hdac1, and Tet proteins. This is consistent with Ogt being one of the most abundant proteins in Tet1 and Tet2 purifications (data not shown).

In order to validate the MS results, we performed an independent Streptavidin purification in fbio-Ogt-expressing BirA ESCs and confirmed that Ogt coprecipitated endogenous Tet1 and Tet2 as well as Hcfc1 and Sin3a (Figure 1E). Moreover, using specific antibodies for Ogt, Tet1, and Tet2 in immunoprecipitations (IPs) with protein extracts prepared from normal growing pluripotent E14 ESCs, we demonstrated that endogenous Tet1 and Tet2 associate with endogenous Ogt in ESCs (Figures 2A–2C, and S1B, and S1C). In addition, the reciprocal coIPs between Tet1 and Tet2 observed in Figures 2A and 2B further suggest a physical connection between these proteins. Remarkably, Tet1 IPs performed on nuclear extracts prepared from ESCs depleted of Ogt expression by transfection of

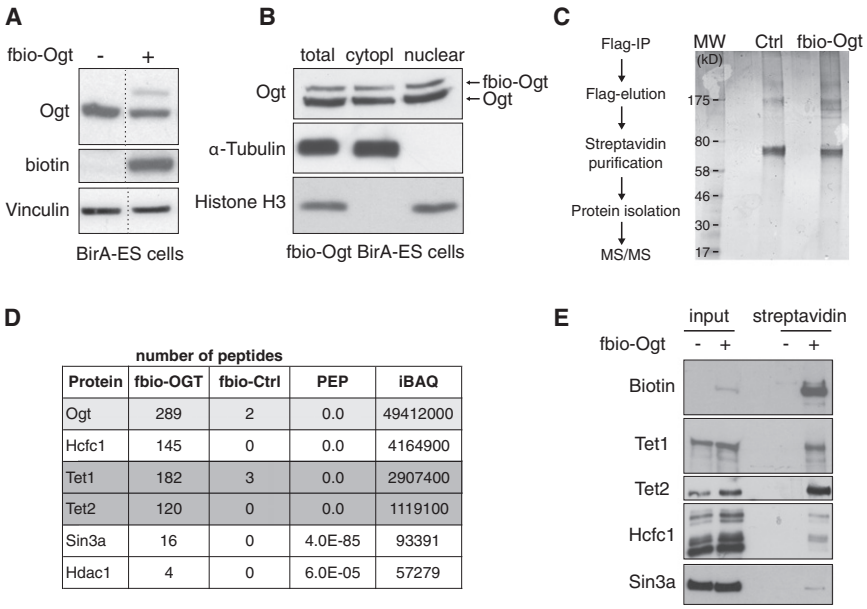

Protein	fbio-OGT	fbio-Ctrl	PEP	iBAQ
Ogt	289	2	0.0	49412000
Hcfc1	145	0	0.0	4164900
Tet1	182	3	0.0	2907400
Tet2	120	0	0.0	1119100
Sin3a	16	0	4.0E-85	93391
Hdac1	4	0	6.0E-05	57279

Figure 1. Nuclear Ogt Stably Purifies with Tet Proteins in Mouse ESCs

(A) Western blot (WB) analyses with the indicated antibodies of protein extracts obtained from BirA-expressing ESCs with (+) or without (–) fbio-Ogt expression. Vinculin served as loading control.

(B) WB of cytoplasm versus nuclear fractionation with the indicated antibodies in fbio-Ogt-expressing BirA ESCs. α-tubulin and histone H3 are presented as fractionation controls.

(C) Scheme of the purification procedure and silver staining of 10% of the eluted proteins from tandem purifications with control or fbio-Ogt-expressing BirA ESCs.

(D) Table of the most relevant proteins identified by mass spectrometry showing the number of peptides detected in both control or fbio-Ogt purifications together with the posterior probability error (PEP) and the intensity based absolute quantification score (iBAQ) determined with MaxQuant.

(E) WB using the indicated antibodies of Streptavidin purifications from protein extracts obtained from fbio-Ogt expressing (+) or not expressing (–) BirA ESCs.

See also Figure S1.

endoribonuclease-prepared small interfering RNAs (esiRNA), showed loss of Tet1-Tet2 interaction upon depletion of Ogt expression (Figure 2D).

To test whether Tet proteins and Hcfc1 coexist together in a complex with Ogt, we fractionated ESC nuclear extracts on size-exclusion chromatography and showed by western blot analyses that Tet1, Tet2, Ogt, and Hcfc1 coelute in high-molecular-weight fractions, consistent with being part of large multiprotein complexes (Figure 3A). Thus, we performed parallel coIP analyses on ESCs nuclear extracts using antibodies specific for Tet1, Tet2, Ogt, Hcfc1, and Sin3a (Figure 3B). The result of this analysis, also summarized in the table presented in Figure 3C, confirms a strong interaction of Tet1 and Hcfc1 with Ogt while depicting a weak interaction between Tet1 and Hcfc1. This result strongly suggests that Tet1 and Hcfc1 form two distinct Ogt containing complexes that can still be in contact with each other. Finally, using a wheat germ agglutinin (WGA) agarose resin to allow isolation of glycoproteins under denaturing conditions (Figure 3D), we demonstrated that, together with Hcfc1 and Ogt itself (two known Ogt substrates), Tet1, Tet2, and Sin3a are enriched on the WGA resin, suggesting that Ogt binding to Tet1 and Tet2 induces their O-GlcNAcylation (Figures 3E and S1D). Such result is consistent with Tet1 being identified in a proteomic approach among nuclear ESC O-GlcNAcylated proteins (Myers et al., 2011). Taken together, these results demonstrate that Tet1 and Tet2 are physiological stable partners of Ogt in the nucleus of ESCs and that they are targets of its enzymatic activity.

Ogt Associates with TSSs of Protein-Coding Genes and Affects Metabolic and Signaling Pathways

In order to determine regions of Ogt association throughout the ESC genome, we performed chromatin immunoprecipitation analyses coupled to high-throughput DNA sequencing (ChIP-seq) with an Ogt-specific antibody. Such experiments led to the identification of 11,552 Ogt binding sites (Table S1). Annotation of these sites enriched for genomic regions that are classified as promoters, introns, and exons (Figure 4A). In addition, the annotation of Ogt binding sites in respect to gene promoters, defined as a 5 kilobase (kb) window over RefSeq annotated transcription start sites (TSSs), shows that 62% of Ogt binding sites are found within promoter regions (Figure 4B). Importantly, the distribution of the density of Ogt binding within a window of 20 kb around RefSeq TSSs showed that Ogt ChIP-seq signals distribute in close proximity to TSS of protein-coding genes (Figure 4C). Overall, these data show that Ogt has a genome-wide preferential association at gene promoters with a precise accumulation in correspondence of their TSSs.

To test whether Ogt activity affects transcription, we decided to set up a strategy to deplete Ogt expression from ESCs. Due to the requirement of Ogt activity for ESC viability (Shafi et al., 2000), we took advantage of esiRNA to transiently knock down Ogt expression. As shown in Figure 4D, esiRNA directed toward *Ogt* led to an efficient downregulation of Ogt expression and to a global loss of protein O-GlcNAcylation. Importantly, transient Ogt depletion did not alter the expression of Tet proteins and did not result in loss of the self-renewing capacity of ESCs, as depicted by the stable expression of pluripotency markers such as Oct4 and Nanog (Figure 4D). Transcriptome analyses led to the identification of 1056 genes that are affected in expression upon downregulation of Ogt expression (Table S2). Ogt-dependent deregulation of gene expression includes a similar number of genes being up- or downregulated (Figure 4E). The microarray expression data of genes with different regulation levels were also independently validated by real-time quantitative PCR (qPCR) analyses (Figure 4F). Functional annotation with ingenuity pathway analysis (IPA) of Ogt-regulated genes revealed a strong increase in the expression of genes involved in glycan biosynthesis and glycerolipids metabolism (Figure 4G). The downregulated genes were enriched for genes involved in

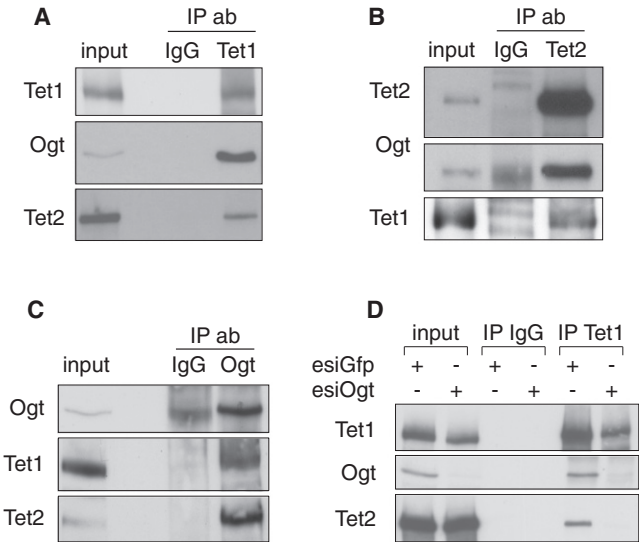

Figure 2. Endogenous Ogt Interacts with Tet1 and Tet2

(A–C) WB with the indicated antibodies of immunoprecipitated (IP) proteins from nuclear E14 ESCs lysate with Tet1- (A), Tet2- (B), and Ogt- (C) specific antibodies. IgG served as unrelated IP control.

(D) WB with the indicated antibodies of IP proteins with a Tet1-specific antibody from protein lysate of cells transfected for 48 hr with Ogt- and Gfp- (control) specific esiRNAs.

See also Figure S1.

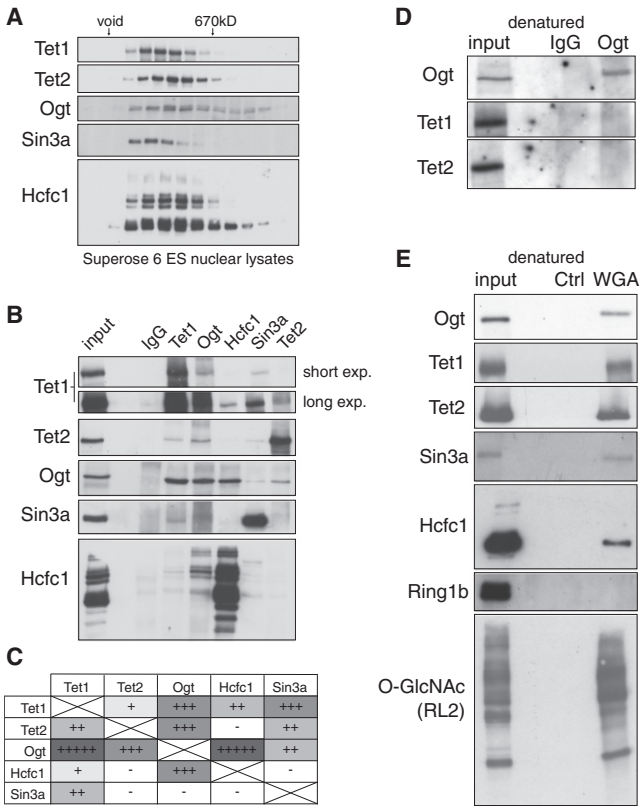

Figure 3. Ogt Forms Distinct Complexes with Tet Proteins and Hcfc1, Mediating Their O-GlcNAcylation

(A) WB with the indicated antibodies on different fractions of E14 ESC nuclear lysates separated on a Superose 6 size-exclusion chromatography.

(B) WB with the indicated antibodies of immunoprecipitated proteins from nuclear E14 ESC lysates with Tet1-, Ogt-, Hcfc1-, Sin3a-, and Tet2-specific antibodies. IgG served as unrelated IP control.

(C) Table summarizing the strength of interaction in the IPs presented in (B).

(D) WB with the indicated antibodies of IP proteins from denatured E14 ESC lysates. IgG is presented as unrelated IP control.

(E) WB with the indicated antibodies of purified proteins with wheat germ agglutinin (WGA) agarose from the denatured E14 ESC protein lysates presented in (D). A nonconjugated agarose resin served as purification control (ctrl).

See also Figure S1.

metabolic signaling pathways and protein biosynthesis (Figure 4G). Importantly, a significant fraction of these genes retains the association of Ogt at their promoter (Figure 4H). Overall, these results show that acute loss of Ogt in ESCs induces transcriptional changes that are consistent with both Ogt enzymatic activity and its pleiotropic functions. Moreover, several of these genes retain Ogt binding at their promoter, suggesting a direct role of Ogt in controlling their expression in agreement with previous *C. elegans* and *D. melanogaster* studies on Ogt nuclear activity (Gambetta et al., 2009; Love et al., 2010).

Ogt and Tet1 Colocalize at Unmethylated CpG-Rich Promoters

Since we have identified Tet1 and Tet2 as stable interacting partners of Ogt in ESCs, we wondered whether Ogt binding to chromatin colocalizes with Tet activity. Tet1 was previously shown in ESCs to bind both at promoters and at distal regulatory elements as well as to overlap with H3K4 trimethylated (H3K4me3) TSSs. Consistent with this, Tet1 binding is found both at promoter and nonpromoter genomic regions (Figure S2A). To test whether Ogt and Tet1 colocalize at the same genomic regions, we overlapped our Ogt data with ChIP-seq analysis for Tet1 and H3K4me3 previously performed in the same ESC line (Mikkelsen et al., 2007; Williams et al., 2011). As shown in the genomic snapshots presented in Figure 5A, Ogt binding seems to perfectly overlay Tet1 ChIP-seq signal at H3K4me3-positive promoters. Consistent with this, more than 90% of Ogt binding sites colocalize with Tet1, and more than 70% of all Ogt peaks show both Tet1 binding and H3K4me3 accumulation (Figure 5B). The colocalization was further validated by real-time qPCR ChIP analyses with a specific Tet1 and two different Ogt antibodies (Figure 5C). Additional analyses with a ChIP-seq data set, generated with a different Tet1-specific antibody (Tet1-C), extend the overlap presented in Figure 5B showing that 98% of Ogt binding sites overlap with Tet1 (Figure S2B). This is consistent with the accumulation of the Ogt and Tet1 ChIP-seq signals at Tet1- and Ogt-unique binding sites identified in Figure 5B (Figure S2C). Tet1 and Ogt colocalization at these sites was further validated by real-time qPCR ChIP analyses (Figures S2D and S2E), and the specificity of these analyses demonstrated by Tet1 and Ogt loss of function experiments (Figures S3A–S3F). Moreover, Ogt also displays a broad overlap with Sin3a binding sites that is in agreement with our interaction data (Figures S4A–S4D). Importantly, analysis of the coverage between Ogt and Tet1 peaks showed a high degree of overlay (80%–100%) that is consistent with their physical interaction (Figure S4E).

The genomic snapshots presented in Figure 5A also suggest that Ogt and Tet1 binding could preferentially occur at promoter regions. To test this, we have annotated all Tet1 binding sites that overlap (+Ogt) or do not overlap (–Ogt) with an Ogt peak (left graph) or, vice versa, the Ogt binding sites that do or do not overlap with Tet1 occupancy (right graph) in relation to RefSeq TSSs. This analysis demonstrated that Tet1 and Ogt colocalization preferentially occurs at the TSSs and not at distal regulatory elements (Figure 5D). A similar analysis, taking CpG-rich islands (CpGis) into account, shows a preferential colocalization of Tet1 and Ogt at CpG-rich genomic regions that is consistent with their preferential coassociation at gene promoters (Figure 5E).

CpG-rich DNA elements are mainly localized at promoter regions and are in general maintained free of DNA methylation. The protection of CpGis from DNA methylation is controlled by the H3K4me3-dependent inhibition of de novo DNA methyltransferases (Hashimoto et al., 2010). While Tet1 binding at distant regulatory elements correlates with 5hmC deposition, Tet1 binding at CpG rich promoters correlates with lack of these DNA cytosine modifications. Indeed, the Ogt ChIP-seq signal increases together with CpG density, and it correlates with lack of 5hmC (Figures 5F and 5G). By generating single-base methylome analyses of ESCs, recent data have identified genomic regions that present low levels of DNA methylation (~30%) and have been characterized as CpG-poor regulatory elements (LMRs) (Stadler et al., 2011). 5hmC in particular accumulates at LMRs (Stadler et al., 2011; Williams et al., 2011), and LMRs are also positive for Tet1 binding. Consistent with our data, the Ogt ChIP-seq signal is reduced from these elements, while it is increased at unmethylated regions (UMRs) and negatively correlates with 5hmC deposition (Figure 5H). These data show that, consistent with their biochemical interaction, Ogt DNA association occurs preferentially at Tet1 binding sites within CpG dense regions that do not contain detectable levels of DNA cytosine modifications.

Tet1 Is Required for Ogt Recruitment to Promoters

Our ChIP data show that Ogt binding to chromatin is significantly decreased in absence of Tet1, suggesting that Tet1 could link Ogt association to DNA. To test this, we decided to isolate proteins from the chromatin-associated fraction of ESCs that stably express *Tet1*-specific short hairpin RNAs (shRNAs). Since decrease of Tet1 only leads to a partial locus-specific reduction of 5hmC levels (Williams et al., 2011), we hypothesized that Tet2 could have redundant functions at Tet1 target sites. Tet2 ChIP analyses at the Tet1-Ogt binding sites were unsuccessful (data not shown), suggesting either that Tet2 does not stably localize at these genomic regions or that our Tet2 antibody is not efficient for ChIP analyses. However, to avoid potential Tet2 compensatory effects, we knocked down Tet2 expression in Tet1 shRNA-interfered ESCs (Figure 6A). WB analyses of chromatin-associated proteins from ESCs depleted for Tet1 and Tet2 showed a strong reduction of Ogt association to chromatin (Figure 6A). Consistent with this, immunofluorescence (IF) staining with Ogt-specific antibodies (Figure S5A) highlighted an increased cytoplasmic distribution of Ogt in Tet1 and Tet2 knockdown cells (Figure S5B). Interestingly, our fractionation analyses presented in Figure 6A also indicate that Tet2, despite localizing in the ESC nucleus (Figure S5C), is poorly associated to chromatin and preferentially accumulates in the soluble fraction (Figure 6A). This suggests that Tet2, differently from Tet1, is loosely associated to chromatin. This observation potentially explains our unsuccessful Tet2 ChIP results and further suggests that Tet2 might not be directly involved in regulating the association of Ogt with chromatin. To test this, we specifically knocked down Tet2 expression in ESCs and demonstrated that Tet1 and Ogt chromatin association was unaltered in absence of Tet2 expression (Figure 6B). Thus, to test whether Ogt chromatin association is only dependent on Tet1 activity, we performed chromatin fractionation analyses in two different Tet1-interfered ESC lines and showed that reduced Tet1 expression induces a global loss of Ogt chromatin association (Figure 6C). Interestingly, loss of Tet1 further reduces the amount of chromatin bound Tet2, suggesting that Ogt-Tet2 interaction could stabilize Tet2 association to chromatin (Figure 6C). To provide further evidence that Ogt promoter association is dependent on Tet1 activity, we performed ChIP analyses with Ogt-specific antibodies at several target promoters before and after depletion of Tet1 expression. Such analyses demonstrated that loss of Tet1 expression displaces Ogt binding from its target genes (Figures 6D, S3C, and S3F) and increases the expression of Ogt-Tet1 common target genes (Figure S6A). Since Ogt seems to O-GlcNAcylate Tet1 (Figure 3E), we also wondered whether loss of Ogt could affect Tet1 stability to chromatin. Indeed, fractionation analyses in Ogt knockdown ESCs revealed a destabilized Tet1 association to chromatin (Figure 7A) that is consistent with its diminished binding at some target promoters observed by ChIP analyses (Figure 7B). However, in absence of Ogt activity, we observed increased 5hmC levels at different Tet1 binding sites (Figure 7C). Such an increase occurs prevalently at promoter regions with low 5hmC and high Ogt levels (Figures 5F–5H), suggesting that loss of Ogt activity promotes 5hmC accumulation. Consistent with this, stabilization of O-GlcNAcylation by inhibition of OGA activity with PUGNAc (Figure S6B) results in decreased 5hmC levels at the same loci (Figure 7D). Overall, these data show that Tet1 mediates global Ogt recruitment to chromatin and that Tet1 interaction with Ogt further stabilizes Tet1 binding at its target promoters, regulating 5hmC levels.

DISCUSSION

Our results demonstrate the existence of a stable complex between the O-GlcNAc transferase Ogt and two components of the 5mC hydroxylase protein family, Tet1 and Tet2, linking two diverse enzymatic activities to chromatin. The fact that Ogt purification also led to the isolation of Sin3a and Hdac1 (previously identified partners of Tet1), although with a minor number of peptides in respect to Tet proteins and Hcfc1, strongly suggests the existence of a multiprotein complex containing Tet1, Tet2, Ogt, Sin3a, and Hdac1. Such complex contains diverse enzymatic activities that are associated with transcriptional repression. Although we detected weak interactions between Hcfc1 and Tet1, we speculate that Tet proteins and Hcfc1 form distinct complexes with Ogt that are in close contact with each other, possibly due to Ogt multimerization (Kreppel

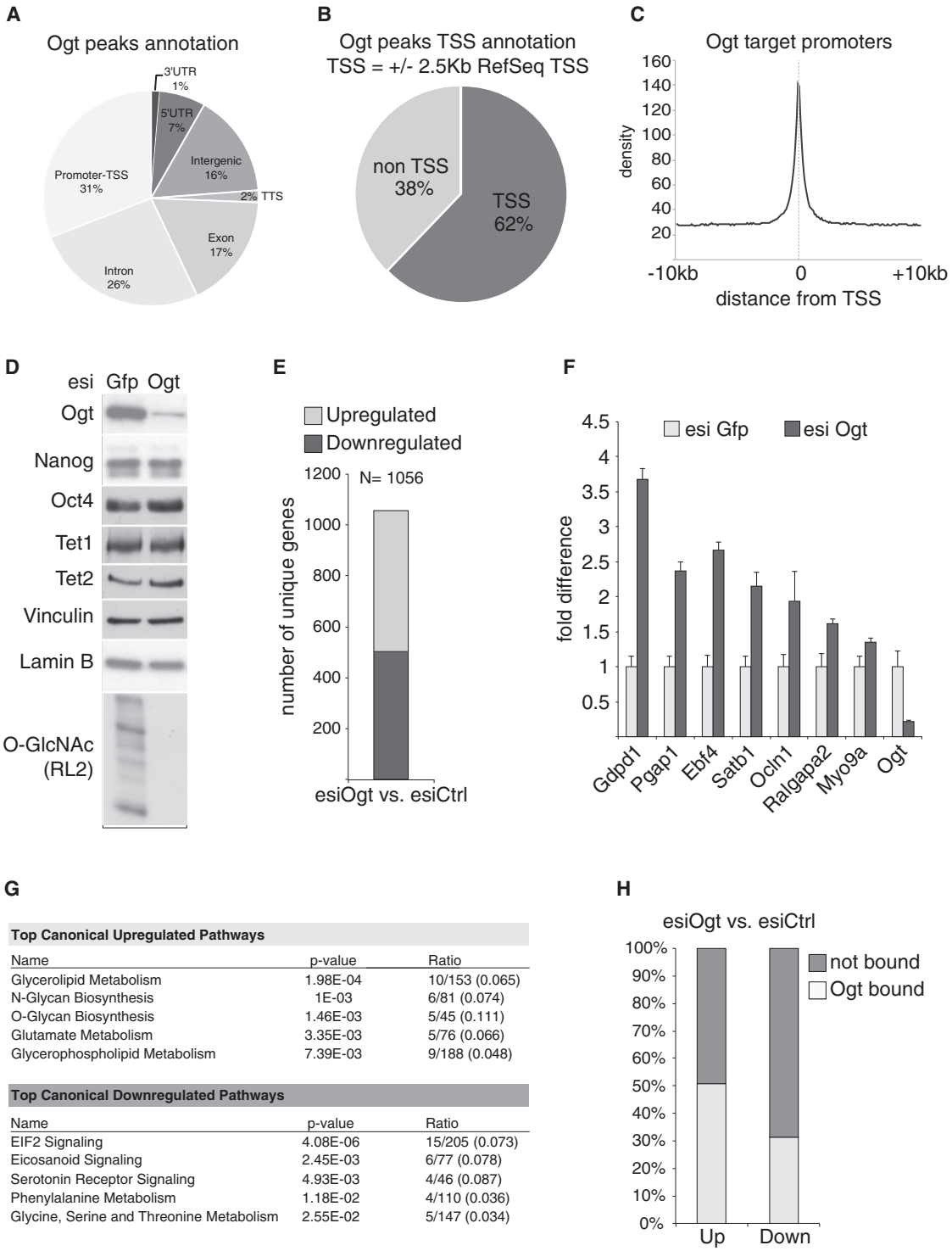

Top Canonical Upregulated Pathways

Name	p-value	Ratio
Glycerolipid Metabolism	1.98E-04	10/153 (0.065)
N-Glycan Biosynthesis	1E-03	6/81 (0.074)
O-Glycan Biosynthesis	1.46E-03	5/45 (0.111)
Glutamate Metabolism	3.35E-03	5/76 (0.066)
Glycerophospholipid Metabolism	7.39E-03	9/188 (0.048)

Top Canonical Downregulated Pathways

Name	p-value	Ratio
EIF2 Signaling	4.08E-06	15/205 (0.073)
Eicosanoid Signaling	2.45E-03	6/77 (0.078)
Serotonin Receptor Signaling	4.93E-03	4/46 (0.087)
Phenylalanine Metabolism	1.18E-02	4/110 (0.036)
Glycine, Serine and Threonine Metabolism	2.55E-02	5/147 (0.034)

Figure 4. Ogt Regulates Metabolic Genes Expression and Associates to TSSs

(A) Ogt peak annotation relative to the indicated genomic feature. Ogt ChIP-seq was performed in E14 ESCs, and peak call was generated by comparison with an unrelated ChIP-seq experiment with rabbit IgG.

(B) Ogt peak annotation relative to genomic regions included within ± 2 kb from RefSeq transcription start sites (TSS).

(C) Density distribution of the Ogt ChIP-seq signals over a window of 20 Kb centered on RefSeq gene TSSs.

(D) Western blot (WB) analyses with the indicated antibodies from protein extracts obtained from E14 ESCs transfected for 48 hr with Gfp- or Ogt-specific esiRNAs. Vinculin and lamin B served as loading controls.

(legend continued on next page)

and Hart, 1999). Interestingly, Hcfc1 was previously shown to interact with distinct domains to both the Sin3a/NURD complex and to the Set1/Ash2 H3K4 methyltransferase complex (Wysocka et al., 2003), suggesting a functional connection between Ogt-Tet association to promoters and the accumulation of H3K4me3 at the same sites. Thus, Ogt seems to have a dual role in binding either Hcfc1 or Tet proteins. While Ogt binding to Hcfc1 has regulatory function on Hcfc1 activity (Capotosti et al., 2011), the fact that loss of Tet1 induces a global displacement of Ogt from chromatin strongly suggests that Tet1 could function as an anchor for Ogt to target promoters, allowing to exert its chromatin related activities.

Ogt chromatin binding preferentially accumulates at the TSSs rather than at Tet1 binding sites located at regulatory elements. This suggests the existence of an additional mechanism that allows Ogt to associate with Tet1 specifically at CpG-rich genomic sites. It is important to note that Tet1 ChIP-seq signal is stronger at CpG-rich sites relative to the CpG-poor elements (Figures 5F and 5G); hence, it is possible that lower sensitivity for Ogt ChIP might result in the lack of significant Ogt detection at these sites as also depicted by real-time qPCR ChIP assays.

Different from Tet1, we found that Tet2 is loosely chromatin associated. This allows the speculation that such difference could be linked with the lack of a CXXC DNA binding domain in Tet2, further suggesting that Tet2 would be placed more distantly respect to Tet1 or Ogt from DNA. This will create a reduced efficiency for simultaneous Tet2 formaldehyde cross-linking with the DNA that could be consistent with our failure in obtaining efficient Tet2 ChIP results. While the weak interaction that we have observed between Tet1 and Tet2 could suggest that Ogt functions as a bridge between these proteins, the independence between Tet1 and Tet2 in maintaining 5hmC levels (Dawlaty et al., 2011; Koh et al., 2011; Williams et al., 2011; Wu et al., 2011a; Xu et al., 2011) strongly suggests the existence of a Tet1-independent mechanism that regulates Tet2 activity. Based on our results, interaction with Ogt occurs preferentially at unmethylated CpG-rich promoters, suggesting that the maintenance of 5mC hydroxylation mediated by Tet1 and Tet2 should take place independently from Ogt. This is consistent with the dual activity of Tet1 in regulating promoter function and genome-wide diffused 5hmC (Dawlaty et al., 2011; Koh et al., 2011; Williams et al., 2011; Wu et al., 2011a; Xu et al., 2011). Nevertheless, local increase in 5hmC levels upon Ogt depletion suggests that increased accumulation of Ogt at specific sites is required to maintain low 5hmC levels.

Considering that Ogt genomic association is localized preferentially at TSSs, Ogt might have a role in transcriptional regulation. In support of this, downregulation of Ogt expression led to both activation and repression of several genes involved in important metabolic and signaling pathways. Considering the pleiotropic function of Ogt in both the cytoplasm and in the nucleus and its tight requirement for ESC viability, it is a big challenge to determine a direct or indirect role in regulating transcription. However, a substantial number of Ogt regulated genes retains the physical association of Ogt at their TSSs. This occurs preferentially for upregulated genes, suggesting that direct Ogt binding at promoters could inhibit transcription. Such observation is consistent with previous reports for Tet1 (Williams et al., 2011; Wu et al., 2011b), as well as with the presence of repressive complexes potentially associated with Ogt at Tet1 binding sites. This activity could involve different chromatin modifications as well as previously reported O-GlcNAcylation of the RNA pol II CTD. However, several genes that retain Ogt binding at their TSSs are downregulated upon loss of Ogt expression suggesting that Ogt could have dual functions in stimulating transcription. This is consistent with both previous reports on Tet1 activity and the role of Ogt in regulating H2Bubq through the GlcNAcylation of H2B S112 (Fujiki et al., 2011). Finally, since Ogt activity seems to stabilize Tet1 at CpG rich sites, it is also possible that Ogt might play alternative roles at promoters. For example, Ogt could act in concert with Tet1 in maintaining CpG-rich promoters free of methylation with mechanism that involves Tet proteins O-GlcNAcylation.

The lack of evident developmental phenotypes in *Tet1* KO mice (Dawlaty et al., 2011) could suggest that the dramatic effects observed in *Ogt* KO embryos are not due to its chromatin-related activities. Although *Tet1* and *Tet2* double-KO mice have not been published, it is possible that requirement of Ogt for general cell viability is related to the cytoplasmic function of Ogt. Our transcriptome analyses showed a marked transcriptional deregulation of key metabolic and signaling pathways. Among the most upregulated pathways, we have identified the synthesis of glycans, a metabolic pathway that generates cofactors for Ogt activity. These results are in agreement with previous findings in *Caenorhabditis elegans* (Love et al., 2010) strongly suggesting that the global reduction of proteins O-GlcNAylation in Ogt depleted ESCs likely activates a strong metabolic response that induces transcriptional changes aimed to restore correct O-GlcNAylation levels. Consistent with this, deregulated expression of the same metabolic and signaling pathways were not observed in Tet1 knockdown ESCs (Williams et al., 2011).

Finally, Ogt could also interact with Tet3. Tet3 is not expressed in ESCs, while it is primarily expressed in the early postfertilization phases of the zygote and has a primary role in regulating reprogramming in embryogenesis affecting proper embryonic development. Bursts of its activity allow global DNA 5mC

(E) Results of the expression analyses of two independent esiRNA experiments performed as in (D) displaying the total number of genes up- or downregulated ($\geq$1.3-fold) upon transient Ogt knockdown.
(F) Real-time quantitative PCR analyses of RNA extracted from an independent esiRNA knockdown experiment performed as in (D) with specific primers for the indicated genes. Data are represented as mean ± SEM.
(G) Ontological classification of upregulated (top panel) and downregulated (bottom panel) genes identified by the analyses presented in (E) with IPA.
(H) Annotation of the Ogt peaks identified in the ChIP-seq analyses shown in (B) relative to the promoters of the upregulated (up) or downregulated (down) genes identified in (E).
See also Table S1 and Table S3.

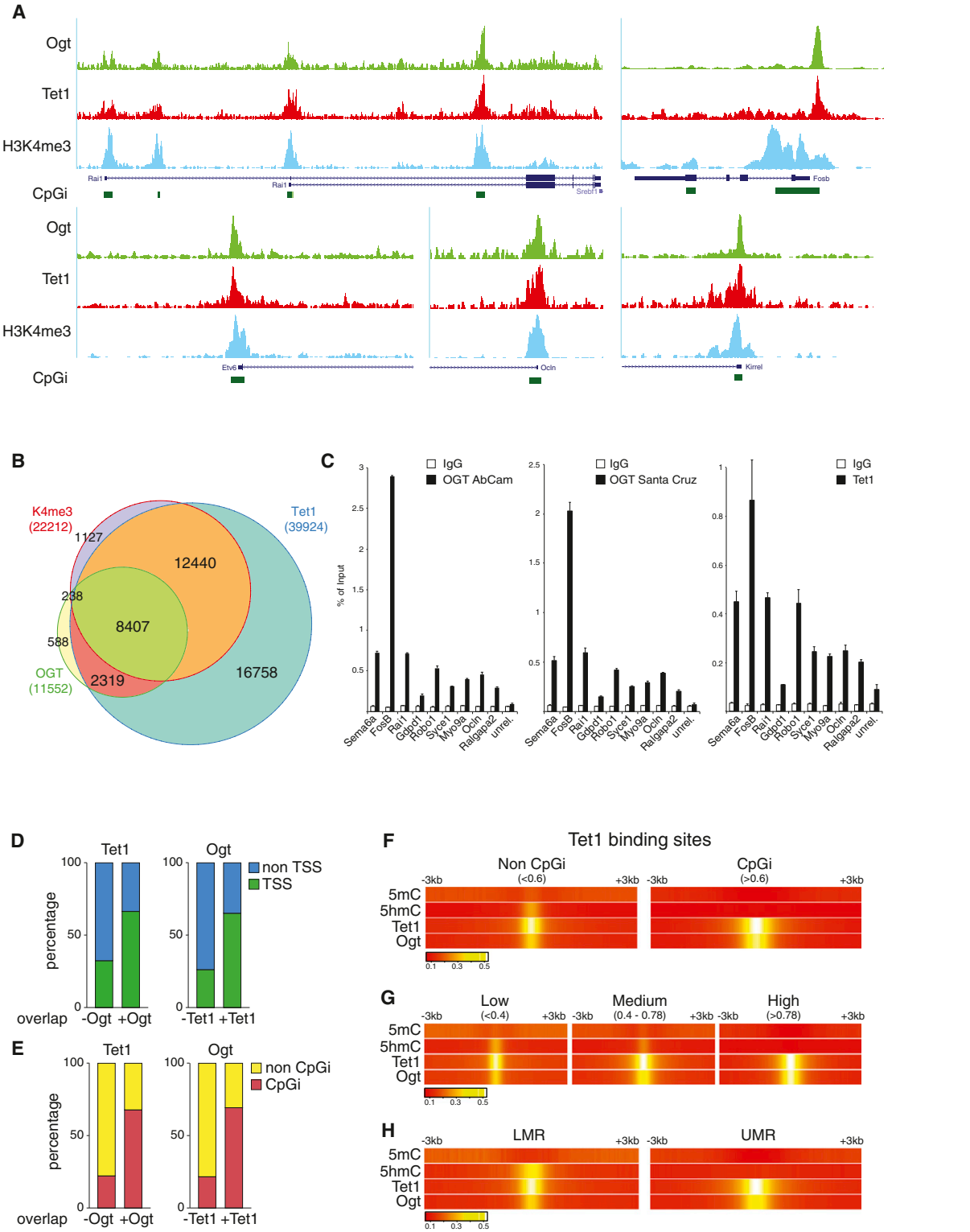

Figure 5. Genome-wide Ogt and Tet1 Colocalization

(A) Genomic snapshots with UCSC genome browser for Ogt, Tet1, and H3K4me3 ChIP-seq results.

(B) Overlap between the genomic positions of the peaks identified in Ogt, Tet1, and H3K4me3 ChIP-seq analyses.

(C) Validation of the ChIP-seq results with Ogt- and Tet1-specific antibodies by real-time quantitative analysis with primers for the indicated antibodies. Data are represented as mean ± SEM.

(legend continued on next page)

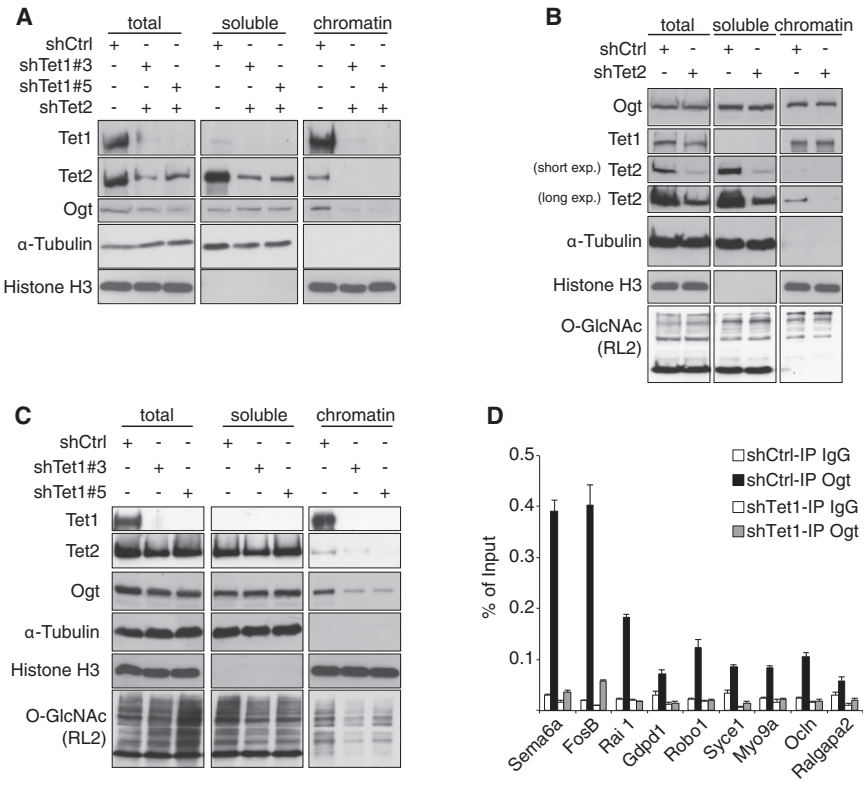

Figure 6. Tet1 Regulates Ogt Binding to Chromatin

(A) Western blot (WB) analyses with the indicated antibodies of E14 ESC-soluble and chromatin-associated proteins that stably express the indicated shRNAs. A scrambled shRNA sequence is used as negative control (shCtrl). α-tubulin and histone H3 are presented as fractionation controls.

(B) WB as in (A) with the indicated antibodies in E14 ESCs stably expressing scrambled (Ctrl) or Tet2-specific shRNAs.

(C) WB as in (A) with the indicated antibodies in E14 ESCs stably expressing scrambled (Ctrl) or Tet1-specific shRNAs.

(D) Real-time quantitative PCR analyses with primers for the indicated gene promoters with DNA purified from ChIP assays. ChIPs were performed with an Ogt-specific antibody in E14 ESCs that stably express scrambled (Ctrl) or Tet1-specific shRNAs. IgG are used as a negative control for ChIP assays. Data are represented as mean ± SEM.

See also Figure S5 and Table S3.

hydroxylation preceding global loss of DNA modification in preimplantation embryos and in primordial germ cells (Gu et al., 2011; Inoue and Zhang, 2011; Wossidlo et al., 2011). In the future, it will be interesting to test whether Ogt can also form a complex with Tet3 and to investigate its role in regulating global 5mC hydroxylation of the paternal pronucleus during embryos reprogramming. Similarly, Tet activity is also present in the mammalian adult brain (Kriaucionis and Heintz, 2009). Considering the strong correlation between Ogt activities, the HSP pathway, and neurodegenerative disorders, it will also be interesting to characterize the role of Ogt-Tet proteins interaction within this context.

Overall, our data identify a protein complex between Ogt and members of the Tet protein family, postulating a mechanism that explains Ogt recruitment to chromatin and further provides evidence for a role of O-GlcNAcylation in stabilizing Tet activity at promoters.

EXPERIMENTAL PROCEDURES

The following sections report essential experimental procedures and reagents information. A full detailed description for all methods is available in the Supplemental Experimental Procedures.

Cell Lines Generation, Manipulation, and Culturing

BirA-expressing ESC clones were generated from an ESC line described elsewhere (Vella et al., 2012). A pCAG-Flag-Avi-Ires-Puromycin vector containing the Ogt coding sequence was used to generate stable integration in BirA ESCs. RNA interference was carried out with esiRNA for Ogt (Sigma-Aldrich, catalog number EMU006701) or for EGFP (Sigma-Aldrich, catalog number EHUEGFP). Tet1 and Sin3a shRNA LKO.1 vectors were described elsewhere (Williams et al., 2011). Tet2 shRNA LKO.1 vector was generated by cloning of the following target sequence: 5′-GCTCTGAACAGTATTCAAAGC-3′. When indicated, cells were treated with PUGNAc (Sigma, catalog number A7229) dissolved in water at a 40 μM final concentration for the indicated time.

Complex Purification, Proteomic Analysis, and Protein Identification

Complex purification and proteomic analyses were carried out essentially as previously described (Vella et al., 2012). A detailed description of the procedure can be found in the Supplemental Experimental Procedures.

Western Blot Analysis, Immunoprecipitation, WGA Purification, and Fractionation

All IPs and western blot were carried out in high-salt lysis buffer (20 mM Tris-HCl [pH 7.6], 300 mM NaCl, 5% glycerol, 0.2% [v/v] Igepal; Sigma-Aldrich, catalog number CA 630). Histones were extracted in 1% SDS, 9 M urea, 25 mM Tris-HCl (pH 6.8), 1 mM EDTA, and 0.7 M mercapto-ethanol. Size-exclusion chromatography was carried out on a Superose 6 column (GE Healthcare) in high-salt buffer. Protein A sepharose beads (GE Healthcare, catalog number 170780-01) or Streptavidin-coated magnetic beads (Invitrogen, catalog number 656-01) were used for IPs. WGA purification was carried out under denaturing conditions (10 min at 95°C in 0.1 M Tris-HCl [pH 7.6], 2%

(D) Left panel, annotation relative to RefSeq gene TSSs of the Tet1 peaks that colocalize (+Ogt) or do not colocalize (–Ogt) with Ogt. Right panel, annotation relative to the RefSeq gene TSSs of Ogt peaks that colocalize (+Tet1) or do not colocalize (–Tet1) with Tet1.

(E) Annotations as in (D) relative to CpG islands (CpGi).

(F) Heat map of the indicated ChIP-seq signal densities in a window of ± 3 kb centered on the summit of Tet1 peaks respect to CpGis.

(G) As in (F), considering Tet1 binding sites relative to their indicated CpG densities.

(H) As in (F), considering Tet1 binding sites annotated relative to low-methylated regions (LMR) and unmethylated regions (UMR).

See also Figures S2–S4, Table S2, and Table S3.

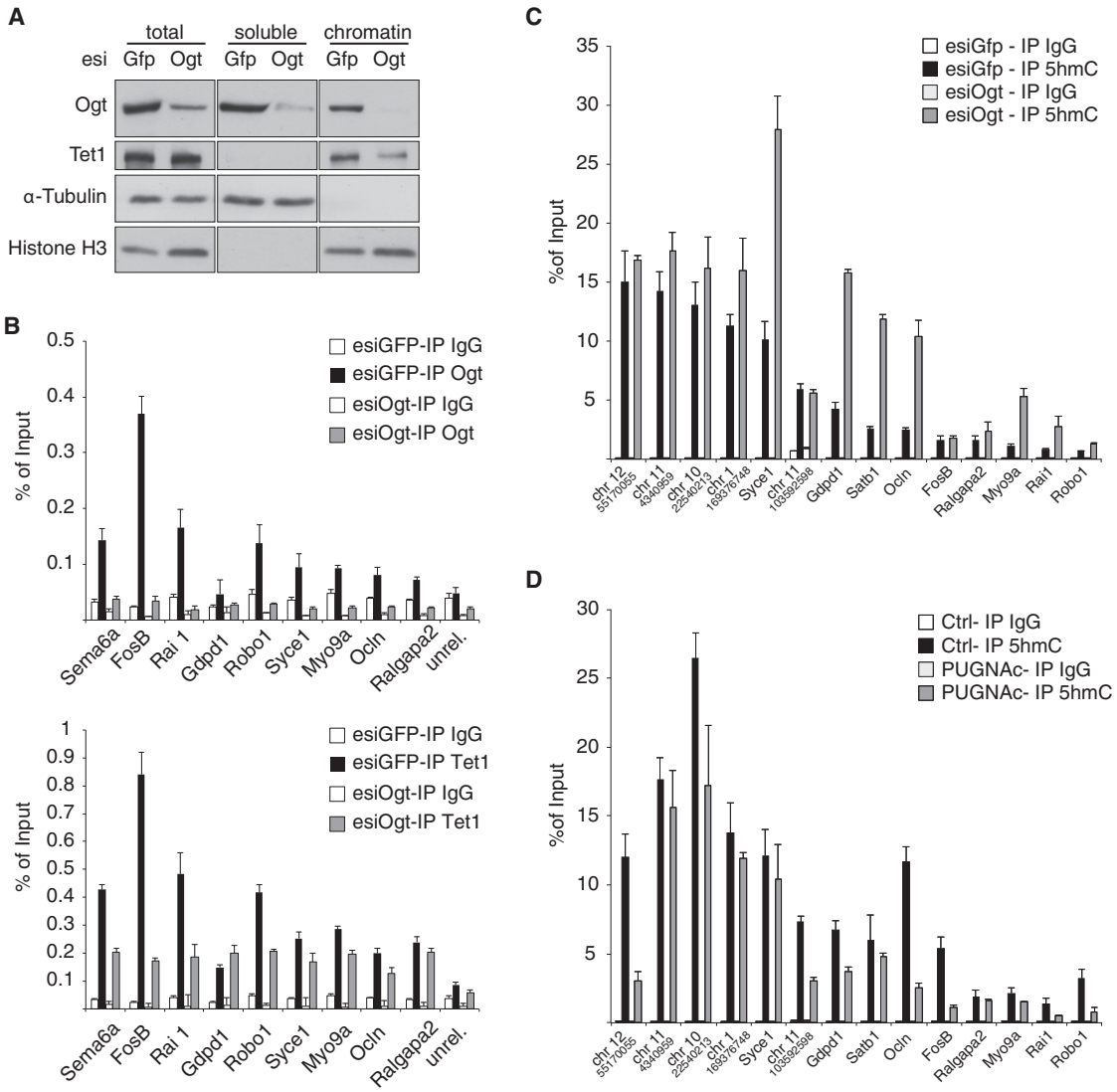

Figure 7. Ogt Regulates Locus-Specific Tet1 Activity

(A) Western blot (WB) analyses with the indicated antibodies of E14 ESC soluble and chromatin-associated proteins in cells transfected for 48 hr with Ogt- and Gfp-specific esiRNAs. α-tubulin and histone H3 are presented as fractionation controls.

(B) Real-time quantitative PCR analyses with primers for the indicated gene promoters with DNA purified from ChIP assays. ChIPs were performed with Tet1- and Ogt-specific antibodies in E14 ESCs transfected for 48 hr with Ogt- and Gfp-specific esiRNAs. IgG are presented as a negative control for ChIP assays. Data are represented as mean ± SEM.

(C and D) Real-time quantitative PCR analyses with primers for the indicated gene promoters and genomic sites (coordinates indicate the central point of PCR amplification) with DNA purified from DIP assays performed with 5hmC specific antibodies on DNA extracted from E14 ESCs transfected for 48 hr with Ogt- and Gfp-specific esiRNAs (C) or treated with 40 μM PUGNAc for 48 hr (D). IgG is presented as a negative control for the DIP assay. Data are represented as mean ± SEM. See also Figure S6 and Table S3.

SDS, and 50 mM DTT) on wheat germ agglutinin resin (Vector Laboratories, catalog number AL-1023S).

ChIP, DIP, and Real-Time Quantitative PCR

ChIP and DIP procedures were carried out as previously described (Pasini et al., 2010; Weber et al., 2005). real-time qPCRs were carried out with Fast SYBR Green (Applied Biosystem). Primers used for PCRs are available in Table S3.

Antibodies

A list of all used antibodies is available in the Supplemental Experimental Procedures.

ChIP-Seq and Microarray Data Analysis

A detailed description of the computational analyses is available in the Supplemental Experimental Procedures. In brief, ChIP-seq data were aligned to the mm9 RefSeq mouse genome, and enriched regions relative to control determined with MACS (Zhang et al., 2008). Only peaks with a p value > 70 were considered for downstream analysis. Raw data from previously published ChIP-seq data sets GSE24843 and GSE12241 were aligned to the mm9 release according to the same criteria. Expression data were generated with Mouse Gene 1.0 ST Affymetrix Arrays and analyzed with Affy and limma bioconductor packages in R (http://www.r-project.org). A probe set with a 1.4-fold expression difference and a p value < 0.05 were considered as differentially expressed.

ACCESSION NUMBERS

Data sets are available for download from NCBI's Gene Expression Omnibus (GEO, http://www.ncbi.nlm.nih.gov/geo/) under accession numbers GSE39154 (ChIP-seq) and Microarrays accession number GSE39321 (microarrays).

SUPPLEMENTAL INFORMATION

Supplemental Information includes Supplemental Experimental Procedures, six figures, and three tables and can be found with this article online at http://dx.doi.org/10.1016/j.molcel.2012.12.019.

ACKNOWLEDGMENTS

We thank Karin Ferrari, Andrea Piunti, Marina Mapelli, Silvia Monzani, and Ulla Toftegaard for technical assistance; Dies Meier for providing the BirA ESCs; and Marianne Pedersen, Paul Cloos, and members of the Pasini laboratory for helpful discussion. The work in the Pasini lab was supported by the Italian Association for Cancer Research and by the Italian Ministry of Health. T.B.'s work was supported by grants from the Giovanni Armenise-Harvard Foundation Career Development Program, the Association of International Cancer Research, the Italian Association for Cancer Research, and the Cariplo Foundation. The work in the Helin lab was supported by grants from the Excellence Program of the University of Copenhagen, the Danish National Research Foundation, the Danish Cancer Society, the Lundbeck foundation, and the Novo Nordisk Foundation. K.H. and J.C. are cofounders of EpiTherapeutics and have shares and warrants in the company.

Received: July 23, 2012
Revised: November 9, 2012
Accepted: December 20, 2012
Published: January 24, 2013

REFERENCES

Booth, M.J., Branco, M.R., Ficz, G., Oxley, D., Krueger, F., Reik, W., and Balasubramanian, S. (2012). Quantitative sequencing of 5-methylcytosine and 5-hydroxymethylcytosine at single-base resolution. Science *336*, 934–937.

Capotosti, F., Guernier, S., Lammers, F., Waridel, P., Cai, Y., Jin, J., Conaway, J.W., Conaway, R.C., and Herr, W. (2011). O-GlcNAc transferase catalyzes site-specific proteolysis of HCF-1. Cell *144*, 376–388.

Chou, T.Y., Hart, G.W., and Dang, C.V. (1995). c-Myc is glycosylated at threonine 58, a known phosphorylation site and a mutational hot spot in lymphomas. J. Biol. Chem. *270*, 18961–18965.

Comer, F.I., and Hart, G.W. (2001). Reciprocity between O-GlcNAc and O-phosphate on the carboxyl terminal domain of RNA polymerase II. Biochemistry *40*, 7845–7852.

Dawlaty, M.M., Ganz, K., Powell, B.E., Hu, Y.C., Markoulaki, S., Cheng, A.W., Gao, Q., Kim, J., Choi, S.W., Page, D.C., and Jaenisch, R. (2011). Tet1 is dispensable for maintaining pluripotency and its loss is compatible with embryonic and postnatal development. Cell Stem Cell *9*, 166–175.

Ficz, G., Branco, M.R., Seisenberger, S., Santos, F., Krueger, F., Hore, T.A., Marques, C.J., Andrews, S., and Reik, W. (2011). Dynamic regulation of 5-hydroxymethylcytosine in mouse ES cells and during differentiation. Nature *473*, 398–402.

Fujiki, R., Hashiba, W., Sekine, H., Yokoyama, A., Chikanishi, T., Ito, S., Imai, Y., Kim, J., He, H.H., Igarashi, K., et al. (2011). GlcNAcylation of histone H2B facilitates its monoubiquitination. Nature *480*, 557–560.

Gambetta, M.C., Oktaba, K., and Müller, J. (2009). Essential role of the glycosyltransferase sxc/Ogt in polycomb repression. Science *325*, 93–96.

Gao, Y., Wells, L., Comer, F.I., Parker, G.J., and Hart, G.W. (2001). Dynamic O-glycosylation of nuclear and cytosolic proteins: cloning and characterization of a neutral, cytosolic beta-N-acetylglucosaminidase from human brain. J. Biol. Chem. *276*, 9838–9845.

Gu, T.P., Guo, F., Yang, H., Wu, H.P., Xu, G.F., Liu, W., Xie, Z.G., Shi, L., He, X., Jin, S.G., et al. (2011). The role of Tet3 DNA dioxygenase in epigenetic reprogramming by oocytes. Nature *477*, 606–610.

Haltiwanger, R.S., Blomberg, M.A., and Hart, G.W. (1992). Glycosylation of nuclear and cytoplasmic proteins. Purification and characterization of a uridine diphospho-N-acetylglucosamine:polypeptide beta-N-acetylglucosaminyltransferase. J. Biol. Chem. *267*, 9005–9013.

Hart, G.W., Slawson, C., Ramirez-Correa, G., and Lagerlof, O. (2011). Cross talk between O-GlcNAcylation and phosphorylation: roles in signaling, transcription, and chronic disease. Annu. Rev. Biochem. *80*, 825–858.

Hashimoto, H., Vertino, P.M., and Cheng, X. (2010). Molecular coupling of DNA methylation and histone methylation. Epigenomics *2*, 657–669.

Hassig, C.A., Fleischer, T.C., Billin, A.N., Schreiber, S.L., and Ayer, D.E. (1997). Histone deacetylase activity is required for full transcriptional repression by mSin3A. Cell *89*, 341–347.

Holt, G.D., and Hart, G.W. (1986). The subcellular distribution of terminal N-acetylglucosamine moieties. Localization of a novel protein-saccharide linkage, O-linked GlcNAc. J. Biol. Chem. *261*, 8049–8057.

Inoue, A., and Zhang, Y. (2011). Replication-dependent loss of 5-hydroxymethylcytosine in mouse preimplantation embryos. Science *334*, 194.

Ito, S., D'Alessio, A.C., Taranova, O.V., Hong, K., Sowers, L.C., and Zhang, Y. (2010). Role of Tet proteins in 5mC to 5hmC conversion, ES-cell self-renewal and inner cell mass specification. Nature *466*, 1129–1133.

Jackson, S.P., and Tjian, R. (1988). O-glycosylation of eukaryotic transcription factors: implications for mechanisms of transcriptional regulation. Cell *55*, 125–133.

Jang, H., Kim, T.W., Yoon, S., Choi, S.Y., Kang, T.W., Kim, S.Y., Kwon, Y.W., Cho, E.J., and Youn, H.D. (2012). O-GlcNAc regulates pluripotency and reprogramming by directly acting on core components of the pluripotency network. Cell Stem Cell *11*, 62–74.

Koh, K.P., Yabuuchi, A., Rao, S., Huang, Y., Cunniff, K., Nardone, J., Laiho, A., Tahiliani, M., Sommer, C.A., Mostoslavsky, G., et al. (2011). Tet1 and Tet2 regulate 5-hydroxymethylcytosine production and cell lineage specification in mouse embryonic stem cells. Cell Stem Cell *8*, 200–213.

Kreppel, L.K., and Hart, G.W. (1999). Regulation of a cytosolic and nuclear O-GlcNAc transferase. Role of the tetratricopeptide repeats. J. Biol. Chem. *274*, 32015–32022.

Kreppel, L.K., Blomberg, M.A., and Hart, G.W. (1997). Dynamic glycosylation of nuclear and cytosolic proteins. Cloning and characterization of a unique O-GlcNAc transferase with multiple tetratricopeptide repeats. J. Biol. Chem. *272*, 9308–9315.

Kriaucionis, S., and Heintz, N. (2009). The nuclear DNA base 5-hydroxymethylcytosine is present in Purkinje neurons and the brain. Science *324*, 929–930.

Love, D.C., and Hanover, J.A. (2005). The hexosamine signaling pathway: deciphering the "O-GlcNAc code". Sci. STKE *2005*, re13.

Love, D.C., Ghosh, S., Mondoux, M.A., Fukushige, T., Wang, P., Wilson, M.A., Iser, W.B., Wolkow, C.A., Krause, M.W., and Hanover, J.A. (2010). Dynamic O-GlcNAc cycling at promoters of Caenorhabditis elegans genes regulating longevity, stress, and immunity. Proc. Natl. Acad. Sci. USA *107*, 7413–7418.

McClain, D.A., Lubas, W.A., Cooksey, R.C., Hazel, M., Parker, G.J., Love, D.C., and Hanover, J.A. (2002). Altered glycan-dependent signaling induces insulin resistance and hyperleptinemia. Proc. Natl. Acad. Sci. USA *99*, 10695–10699.

Mikkelsen, T.S., Ku, M., Jaffe, D.B., Issac, B., Lieberman, E., Giannoukos, G., Alvarez, P., Brockman, W., Kim, T.K., Koche, R.P., et al. (2007). Genome-wide maps of chromatin state in pluripotent and lineage-committed cells. Nature *448*, 553–560.

Myers, S.A., Panning, B., and Burlingame, A.L. (2011). Polycomb repressive complex 2 is necessary for the normal site-specific O-GlcNAc distribution in mouse embryonic stem cells. Proc. Natl. Acad. Sci. USA *108*, 9490–9495.

Pasini, D., Cloos, P.A., Walfridsson, J., Olsson, L., Bukowski, J.P., Johansen, J.V., Bak, M., Tommerup, N., Rappsilber, J., and Helin, K. (2010). JARID2 regulates binding of the Polycomb repressive complex 2 to target genes in ES cells. Nature *464*, 306–310.

Sakabe, K., Wang, Z., and Hart, G.W. (2010). Beta-N-acetylglucosamine (O-GlcNAc) is part of the histone code. Proc. Natl. Acad. Sci. USA *107*, 19915–19920.

Shafi, R., Iyer, S.P., Ellies, L.G., O'Donnell, N., Marek, K.W., Chui, D., Hart, G.W., and Marth, J.D. (2000). The O-GlcNAc transferase gene resides on the X chromosome and is essential for embryonic stem cell viability and mouse ontogeny. Proc. Natl. Acad. Sci. USA *97*, 5735–5739.

Shaw, P., Freeman, J., Bovey, R., and Iggo, R. (1996). Regulation of specific DNA binding by p53: evidence for a role for O-glycosylation and charged residues at the carboxy-terminus. Oncogene *12*, 921–930.

Stadler, M.B., Murr, R., Burger, L., Ivanek, R., Lienert, F., Schöler, A., van Nimwegen, E., Wirbelauer, C., Oakeley, E.J., Gaidatzis, D., et al. (2011). DNA-binding factors shape the mouse methylome at distal regulatory regions. Nature *480*, 490–495.

Tahiliani, M., Koh, K.P., Shen, Y., Pastor, W.A., Bandukwala, H., Brudno, Y., Agarwal, S., Iyer, L.M., Liu, D.R., Aravind, L., and Rao, A. (2009). Conversion of 5-methylcytosine to 5-hydroxymethylcytosine in mammalian DNA by MLL partner TET1. Science *324*, 930–935.

Vella, P., Barozzi, I., Cuomo, A., Bonaldi, T., and Pasini, D. (2012). Yin Yang 1 extends the Myc-related transcription factors network in embryonic stem cells. Nucleic Acids Res. *40*, 3403–3418.

Vosseller, K., Wells, L., and Hart, G.W. (2001). Nucleocytoplasmic O-glycosylation: O-GlcNAc and functional proteomics. Biochimie *83*, 575–581.

Weber, M., Davies, J.J., Wittig, D., Oakeley, E.J., Haase, M., Lam, W.L., and Schübeler, D. (2005). Chromosome-wide and promoter-specific analyses identify sites of differential DNA methylation in normal and transformed human cells. Nat. Genet. *37*, 853–862.

Williams, K., Christensen, J., Pedersen, M.T., Johansen, J.V., Cloos, P.A., Rappsilber, J., and Helin, K. (2011). TET1 and hydroxymethylcytosine in transcription and DNA methylation fidelity. Nature *473*, 343–348.

Williams, K., Christensen, J., and Helin, K. (2012). DNA methylation: TET proteins-guardians of CpG islands? EMBO Rep. *13*, 28–35.

Wossidlo, M., Nakamura, T., Lepikhov, K., Marques, C.J., Zakhartchenko, V., Boiani, M., Arand, J., Nakano, T., Reik, W., and Walter, J. (2011). 5-Hydroxymethylcytosine in the mammalian zygote is linked with epigenetic reprogramming. Nat Commun *2*, 241.

Wu, H., and Zhang, Y. (2011). Mechanisms and functions of Tet protein-mediated 5-methylcytosine oxidation. Genes Dev. *25*, 2436–2452.

Wu, H., D'Alessio, A.C., Ito, S., Wang, Z., Cui, K., Zhao, K., Sun, Y.E., and Zhang, Y. (2011a). Genome-wide analysis of 5-hydroxymethylcytosine distribution reveals its dual function in transcriptional regulation in mouse embryonic stem cells. Genes Dev. *25*, 679–684.

Wu, H., D'Alessio, A.C., Ito, S., Xia, K., Wang, Z., Cui, K., Zhao, K., Sun, Y.E., and Zhang, Y. (2011b). Dual functions of Tet1 in transcriptional regulation in mouse embryonic stem cells. Nature *473*, 389–393.

Wysocka, J., Myers, M.P., Laherty, C.D., Eisenman, R.N., and Herr, W. (2003). Human Sin3 deacetylase and trithorax-related Set1/Ash2 histone H3-K4 methyltransferase are tethered together selectively by the cell-proliferation factor HCF-1. Genes Dev. *17*, 896–911.

Xu, Y., Wu, F., Tan, L., Kong, L., Xiong, L., Deng, J., Barbera, A.J., Zheng, L., Zhang, H., Huang, S., et al. (2011). Genome-wide regulation of 5hmC, 5mC, and gene expression by Tet1 hydroxylase in mouse embryonic stem cells. Mol. Cell *42*, 451–464.

Yang, X., Zhang, F., and Kudlow, J.E. (2002). Recruitment of O-GlcNAc transferase to promoters by corepressor mSin3A: coupling protein O-GlcNAcylation to transcriptional repression. Cell *110*, 69–80.

Yu, M., Hon, G.C., Szulwach, K.E., Song, C.X., Zhang, L., Kim, A., Li, X., Dai, Q., Shen, Y., Park, B., et al. (2012). Base-resolution analysis of 5-hydroxymethylcytosine in the mammalian genome. Cell *149*, 1368–1380.

Zeidan, Q., and Hart, G.W. (2010). The intersections between O-GlcNAcylation and phosphorylation: implications for multiple signaling pathways. J. Cell Sci. *123*, 13–22.

Zhang, Y., Liu, T., Meyer, C.A., Eeckhoute, J., Johnson, D.S., Bernstein, B.E., Nusbaum, C., Myers, R.M., Brown, M., Li, W., and Liu, X.S. (2008). Model-based analysis of ChIP-Seq (MACS). Genome Biol. *9*, R137.